CHAPTER 186

QUASI-TURBULENT BOUNDARY LAYER OF OSCILLATING FLOW OVER RIPPLES

Yukio Sato[1]
and
Ken-ichiro Hamanaka[2]

ABSTRACT

When the surface waves propagate in shallow water region, the bottom boundary layer may be turbulent because of sand ripples or other kind of roughness of sea bed. But before the flow becomes fully developed turbulence, there is a state, in a certain range of the Reynolds number, in which the flow is still laminar but has separation and complex structure of vortex. This is termed as quasi-turburent flow in the present paper. The flow structure of this boundary layer affects the mass transport and sedimataion.

In the present paper, we use a numerical method to solve the boundary layer of oscillatary flow over ripples. When we discuss the overall wave field, the sand ripples can be considered as ruoghness of the bollom and the flow with the separation and the vortex can be considered as disturbance around mean flow. Therefore, to discuss the averaged flow structure of wave field, the mass transport for example, it is necessary to know some kind of statistical properties of the boundary layer. A particular attention is paid to investigate the mean velocity, the Reynolds stress and turbulent viscosity. It is found that the turbulent viscosity varies along the time during the period of the oscillation. And not only it diverses as the space derivative of the mean velocity diminishes, but also it has a complex distribution in space and time.

[1] Associate Professor, Dept. of Civil Eng., Kitami Inst. of Tech., Koen-cho 165, Kitami 090, Japan.
[2] Dr. Eng., Research Associate, Dept. of Civil Eng., Hokkaido Univ., N 13, W 8, Sapporo 060, Japan.

1. INTRODUCTION

Sand ripples are commonly observed on the sea bed in coastal region, which produce complex flow structures near the bed under the influence of the wave motions. This flow structures strongly affect to the development of ripples, the mass transport inside and outside the boundary layer, and the sedimentation near the bed.

In the case where the flow near the bed is fully developed turbulence, Longuet-Higgins(1958) analized the Eularian mean velocity and the mass transport velocity just outside the boundary layer. He concluded that the Eularian mean velocity and the mass transport are independent to the distribution of the turbulent viscosity. In his analysis it is assumed that the local turbulent viscosity is constant along with the time during the wave period. But the validity of this assumption seems to be questionable. Furthermore, when we discuss the mass transport inside the boundary layer, we need to know the distribution of the turbulent viscosity even if Longuet-Higgins' assumption is correct.

On the natural sea bed, the wave length of the ripples is very short compared with that of the surface wave. Therefore to investigate the flow structure inside the boundary layer, horizontally oscillating flow can be considered as a first approximation for the ambient flow. Blondeaux and Vittori(1991) investigated this flow structure in a numerical approach. Hamanaka and Sato(1991) also proposed a similar numerical method independently using the spectral method and the finite differential scheme. Both of them confirmed that their methods describe the separations and large vortex structures.

In the present paper, we use the same numerical method of Hamanaka and Sato(1991) and solve the oscillatory boundary layer on ripples under the quasi-turbulence condition. A particular attention is paid to investigate the mean velocity, the Reynolds stress and the turbulent viscosity on the same flow conditions mentioned above. Spatial averaging procedure is taken over the wave length of ripple. The turbulent viscosity is found to be dependent on time during the period of the oscillating flow. Not only it diverses as the space derivative of the mean velocity diminishes, but also it has a complex pattern of its distribution in space and time. A similar result can be seen in the experimental measurement of Sleath (1987), in the case of fully developed turbulent boundary layer. This fact suggests that Longuet-Higgins' assumption mentioned above is not correct. A example of this incorrectness is seen in the difference between

Tanaka's model and measurement (Tanaka, 1989).

2. FORMULATION OF THE PROBLEM

In the present paper, we follow the same numerical approach of Hamanaka and Sato (1991). We consider two dimensional viscous flow oscillating over a periodic wavy bottom and assume that the wavy bottom vary sinusoidally to the direction of x axis. The vorticity equation and the Poisson equation for the stream function is employed as the governing equation.

$$\omega_t = \phi_x \omega_y - \phi_y \omega_x + \nu (\omega_{xx} + \omega_{yy}) \qquad \text{------------ (1)}$$

$$\phi_{xx} + \phi_{yy} = -\omega \qquad \text{------------- (2)}$$

where, ω^* is vorticity, ϕ^* is stream function and ν^* is kinematic viscosity.
The flow outside the boundary layer is given by

$$u^* = \sigma^* A^* \sin(\sigma^* t^*) \quad , \quad v^* = 0 \qquad \text{--------------- (3)}$$

where, u^* and v^* are horizontal and vertical velocity components outside the boundary layer. And, σ^* is angular frequency, A^* is amplitude of velocity.
A new coordinate system is introduced.

$$x^* = \xi^* - a^* \exp(-k^* \eta^*) \sin(k^* \xi^*)$$
$$\text{-------- (4)}$$
$$y^* = \eta^* + a^* \exp(-k^* \eta^*) \cos(k^* \xi^*)$$

where, k^* and a^* are wave number and amplitude of the ripple respectively. The ripple profile is mapped into the line $\eta^* = 0$.
All variables are nondimensionlized with k^* and σ^*.

$$\xi = k^* \xi^* \quad , \quad \eta = k^* \eta^* \quad , \quad t = \sigma^* t^*$$
$$\text{-------- (5)}$$
$$\phi = \frac{k^{*2}}{\sigma^*} \phi^* \quad , \quad \omega = \frac{\omega^*}{\sigma^*} \quad , \quad \nu = \frac{k^{*2}}{\sigma^*} \nu^*$$

Then, the governing equations (1) and (2) are represented in (ξ , η) coordinate system.

$$\omega_t = J^{-1} \{ -\phi_\eta \omega_\xi + \phi_\xi \omega_\eta + \nu (\omega_{\xi\xi} + \omega_{\eta\eta}) \} \quad \text{-------- (6)}$$

$$\phi_{\xi\xi} + \phi_{\eta\eta} = -J\omega \quad \text{----------- (7)}$$

where, J is the Jacobian of transformation by Eq.(4) :

$$J = 1 - 2a \exp(-\eta) \cos(\xi) + a^2 \exp(-\eta) \quad \text{-- (8)}$$

$$J^{-1} = 1/J$$

The boundary conditions on the bottom are

$$\phi = \phi_\xi = \phi_\eta = 0 \quad \text{on} \quad \eta = 0 \quad \text{----------- (9)}$$

and outside the boundary layer,

$$\phi_\xi \to 0 \ , \ \phi_\eta \to A \sin(t) \ , \ \omega \to 0 \quad \text{at } \eta \to \infty \quad \text{--------(10)}$$

where, $A = k^* a^*$.
The parameters a , A and ν specify this problem.

The parameter a determines the bottom topography. When a is constant, the similarity law suggests two dimensionless numbers, Reynolds number (Re) and Strouhal number (S). Let the representative variable of the length scale be the wave length of the ripple profile (L^*) , the time scale, the period of oscillation (T^*) , and the velocity, the maximum velocity of oscillation ($\sigma^* A^*$), then, Reynolds number (Re) and Strouhal number (S) are described as follows.

$$Re = \frac{\sigma^* A^* L^*}{\nu^*} = 2\pi \frac{A}{\nu} \quad , \quad S = \frac{\sigma^* A^* T^*}{L^*} = A \quad (11)$$

Instead of solving this problem directly, we introduce the Fourier series expansion for ϕ and ω along the axis ξ ,

$$\phi = \Sigma f_m \exp(im\xi) \quad , \quad \omega = \Sigma g_m \exp(im\xi) \quad \text{------(12)}$$

Substituting (12) into (7) , we obtain equation (13).

$$\frac{\partial^2 f_m}{\partial \eta^2} - m^2 f_m = -H_m \quad \text{----------- (13)}$$

where, $J\,\omega = \Sigma\,H_m\,e^{im}$

        In general, there can be considered two way to treat the
vorticity equation. When the wave number space (Fourier coefficients)
is used, the convolution sum is needed to calculate the nonlinear
terms. And when the physical space is used, the inverse Fourier
transform is needed in each time step. In the present paper, the
latter method is used.
        We introduce a new coordinate system in which finer meshes
can be defined near the bottom, and coarser ones in the upper
region.

$$\eta = \eta_T \frac{exp\,(b\,\zeta)\;-1}{exp\,(b)\;-1} \qquad\qquad\qquad \text{------------ (14)}$$

The boundary condition for (12) is on the bottom

$$f_m = 0 \quad on \quad \zeta = 0 \qquad\qquad \text{-------------- (15)}$$

and outside the boundary layer

$$\frac{\partial\zeta}{\partial\eta}\,\frac{\partial f_m}{\partial\zeta} = \begin{array}{ll} A\,sin(t) & ,\quad m=0 \\ 0 & ,\quad m\neq 0 \end{array} \quad on \quad \zeta = 1 \qquad (16)$$

for the vorticity equation

$$\omega = 0 \quad on \quad \zeta = 1 \qquad\qquad \text{-------------- (17)}$$

        The vorticity on the upper boundary is assumed to be zero,
and on the bottom it is given by Thom's scheme with the bottom
condition of the stream function (Roache 1972).

$$\omega = -\,J^{-1}\,(\frac{\partial\zeta}{\partial\eta})^2\;\frac{2\,\phi\,(\triangle\zeta)}{\triangle\zeta} \qquad on \quad \zeta = 0 \quad \text{------------ (18)}$$

3. NUMERICAL PROCEDURE

        The equation (6) and (13) are solved numerically by use of a
forward difference scheme for the time derivative, and a central
difference scheme for the spatial derivative. The vorticity at new
time step is obtained through (6) with three inverse Fourier
transform in the right hand side of the equation. The Fourier

coefficient of the stream function is obtained through (13) with Fourier transform of the right hand side. Then, the vorticity on the bottom is obtained through (18). In this procedure, Fourier transform and inverse Fourier transform are needed but FFT algorithm may be available in any computer system.

In this paper, the parameters a and A are fixed on 0.5 and 5.0, and several calculations is carried out with the several different value of ν. The value of A is selected as the moving distance of water particles by oscillating flow becomes to a wave length of the ripple. The computation starts from the fluid at rest.

Table 1. gives the computational conditions which are discussed in this paper. M and N are the numbers of grids on ξ-axis and ζ-axis respectively. NT is time step number of one period of the oscillation.
Therefore, the time step $\triangle$ t becomes

$$\triangle t = 2 \pi \diagup N T$$

RUN	M	N	η_T	b	a	A	ν	Re	NT	cycle
4	64	32	5	3	0.5	5	0.05	630	3200	3
23	64	90	7	3	0.5	5	0.03	1050	12000	5
27	64	90	10	3	0.5	5	0.02	1570	12000	6

Table 1. Computational conditions

4. DISCUSSION OF RESULTS

In this problem , three nondimentional parameters a , A and ν specify the flow. In the present calculations, a and A are fixed while ν takes different values as shown in the table 1. This means the Strouhal number remains constant while the Reynolds number varies in the different cases. The flow with these conditions can be confirmed to be stable from the experimental measurements by Du Toit and Sleath (1981).

Fig. 1 shows the contours of vorticity of the flow with the condition of RUN 4 in the table 1, after three cycles from the rest. (a)-(h) in Fig. 1 correspond to the eight successive phases in one cycle. The fluid outside the boundary layer flows from the left to the right during the first half cycle and reverses during the next

half cycle. The bold lines show the positive vorticity (counter-clockwise) and the fine lines show the negative one (clockwise). The ambient flow is accelerated in (a), takes maximum velocity in (b), is decelerated in (c) and rests in (d).

Fig. 2 shows the contours of stream function of the same flow of Fig. 1. It is found that both the separation on the lee side of the crest and the large vortex shed from the bottom are well described in this numerical method. In Fig. 1 and Fig. 2, corresponding flows in each half cycle ((a)-(e) and (b)-(f) etc.) are almost symmetric. This means that almost stationary oscillating flow is obtained. Furthermore, in the phase of the deceleration larger separation structure is formed than in the acceleration phase. When the ambient flow reverses its direction, a cloud of vorticity is shed from the bottom and drifts with the ambient flow diminishing the intensity of its vorticity.

As mentioned in the section 1, the wave length of the ripples is very short compared with that of the surface wave in normal coastal region. Therefore the ripples can be considered as bottom roughness. In this sense, it would be reasonable to investigate the Reynolds stress and the turbulent viscosity for mean flow. In general, the averaging procedure can be taken in time, in phase or in space. But to investigate Longuet-Higgins' assumption mentioned in section 1, it will be suitable to use the spatial averaging procedure where the mean velocity is calculated from the averaged velocity over a wave length of the ripple. Then, the Reynolds stress R_y and the turbulent viscosity ν_T are given by,

$$R_y = -<u' \, v'> \qquad \text{--------------- (21)}$$

$$\nu_T = -<u' \, v'> \bigg/ \frac{d \, U}{d \, y} \qquad \text{--------------- (22)}$$

where

$$u = U + u' \ , \ U = <u> \qquad \text{--------------- (23)}$$

and < > denotes the average over a wave length.

Fig. 3 shows the distribution of the mean horizontal velocity of RUN 4.   Fig. 4 and Fig. 5 show the distribution of the Reynolds stress and the turbulent viscosity of the same flow .   From Fig. 5, the turbulent viscosity is found to vary its value during the period of oscillation. And not only it has complex distributions but also diverges in different ways (in positive or negative) as the space derivative of mean velocity is diminishes. A similar result can

be seen in the experimental measurement in the case of fully developed turbulent boundary layer (Sleath,1987).

Fig. 6 shows the contours of vorticity in the case of RUN 23. Comparing with Fig. 1, it is found that when the Reynolds number increases the intensity of vorticity becomes higher and its distribution gets much more complexity and the cloud of vortex drifts longer time with the ambient flow.

Fig. 7 and Fig. 8 show the mean velocity and the Reynolds stress of the flow of Fig. 6.

The fundamental characteristics are the same of those of RUN 4. But it can be seen from these figures that the phase shifts in the mean velocity and the Reynolds stress appears at much higher position because of the development of the boundary layer. The turbulent viscosity of this flow also has the same characteristics of RUN 4.

Let us discuss the detail of time dependence of the characteristics of boundary layer. Fig. 9(a) shows the contours of mean velocity of RUN 4 during one cycle. The bold lines denote the positive contours and the fine ones, negative ones. The height at which the mean velocity takes the maximum at each phase rises up lineally with time in each half cycle. A similar result can be seen in the turbulent intensity of fully developed turbulent oscillatory flow from the experimental measurement by Sleath (1987).

Fig. 9(b) shows the contours of the Reynolds stress of RUN 4. The Reynolds stress has two peaks in each half cycle and its intensity at the acceleration phase is higher than that at the deceleration phase.

Fig. 9(c) shows the contours of the turbulent viscosity of RUN 4. The zigzagged line where the positive contour and negative contour are close each other indicates the divergence of the turbulent viscosity. The similar result can be seen in fully developed turbulent flow (Sleath, 1987).

Fig. 10 is for RUN 23 and Fig. 11 is for RUN 27, corresponding to Fig 9 for RUN 4. As expected from the previous discussion, as the Reynolds number increases the distribution of each valuables gets higher complexity. Also it is commonly seen that the turbulent viscosity strongly depends on time and not only it has positive and negative value but also it diverses positive way and negative way. This result suggests that the Longuet-Higgins' assumption is incorrect. A effect of this incorrectness is seen in the difference between Tanaka's model and measurement (Tanaka, 1989). He proposed a turbulent viscosity model which depends only to the height from the

bottom, and estimated the mean velocity in a fully developed turbulent oscillatory flow. Significant differences can be seen around the peak points of the mean velocity distributions.

5. CONCLUSION

The flow structures of oscillatory boundary layer on rippled bottom are investigated in a numerical method. It is confirmed that the turbulent viscosity depends on time and diverses in positive and negative. This suggests that the Longuet-Higgins' assumption is unreasonable and consequently the Eularlan steady flow and the mass transport under the wave motion should be reinvestigated.

REFERENCES

Blondeaux,P. and Vittori,G. (1991) : Vorticity dynamics in an oscillatory flow over a rippled bed, Jour. of Fluid Mech. Vol. 226, pp.257-289

Du Toit,C.G. and Sleath,J.F.A. (1981) : Velocity measurements close to rippled beds in oscillatory flow, Jour of Fluid Mech. Vol. 112, pp. 71-96.

Hamanaka,K. and Sato,Y. (1991): Separation of oscillating flow over a wavy bed, Proc. of Int. Meeting on Hydraulic Transients with Water Column Separation, pp. 156-167

Longuet-Higgins,M.S. (1958) : An experimental investigation of drift profiles in a closed channel, appendix, in Proc. of 16 th Int. Conf. on coastal Eng., ASCE, pp. 184-193.

Sleath,J.F.A. (1987) : Turbulent oscillatory flow over rough beds, Jour. Fluid Mech. Vol. 182, pp. 369-409

Tanaka,H. (1989) : Bottom boundary layer under non-linear wave motion, Jour. of Waterway, Port, Coastal, and Ocean Engineering, ASCE ,Vol. 115, No. 1, pp. 40-57
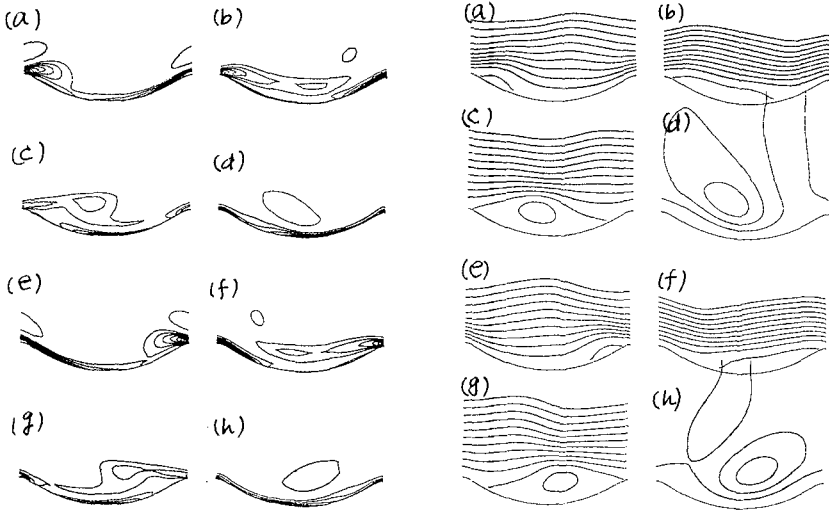
Fig.1 Vorticity contours (Run 4)
$\Delta \omega = 5$

(a):$2\pi*1/8$,(b):$2\pi*2/8$,(c):$2\pi*3/8$,(d):$2\pi*4/8$
(e):$2\pi*5/8$,(f):$2\pi*6/8$,(g):$2\pi*7/8$,(h):$2\pi*8/8$

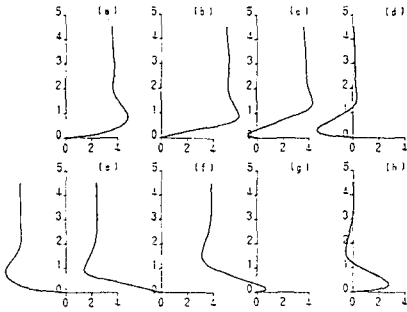Fig.2 Stream function contours
(Run 4) : $\Delta \phi = 5$

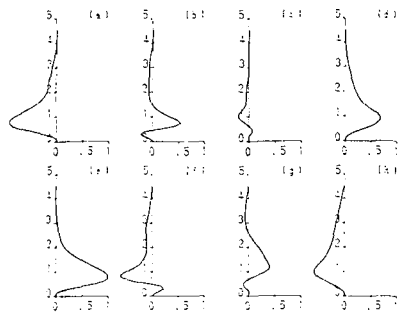Fig.3 Distributions of mean fluid
velocity (U) (Run 4)
(a) ～ (h) see Fig.2

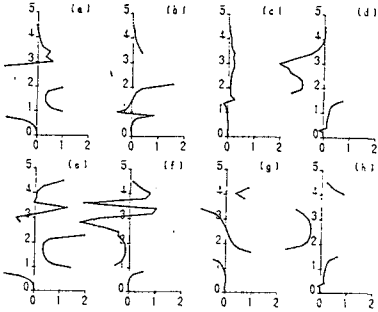Fig.4 Distributions of Reynolds
stress (Ry) (Run 4)
(a) ～ (h) see Fig.2

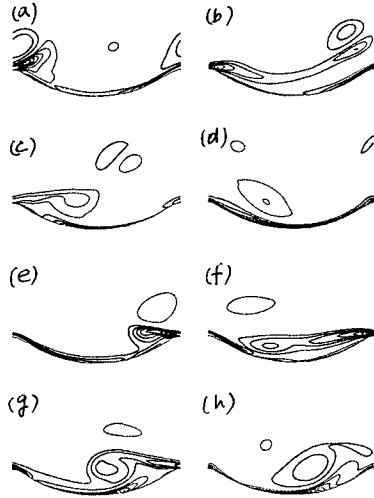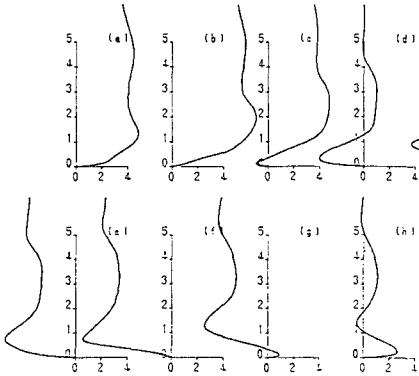Fig.5 Distributions of turbulent
       viscocity (ν_T) (Run 4)
       (a) ~ (h) see Fig.2

Fig.6 Vorticity contours (Run 23)
       $\Delta\ \omega = 5$:(a) ~ (h) see Fig.2

Fig.7 Distributions of mean fluid
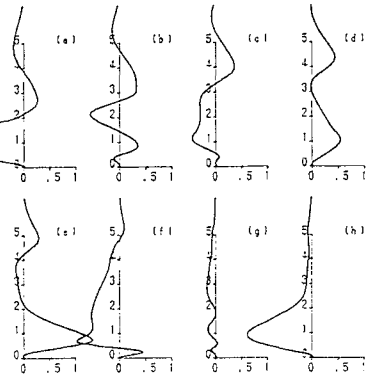   velocity (U) (Run 23)
       (a) ~ (h) see Fig.2

Fig.8 Distributions of Reynolds
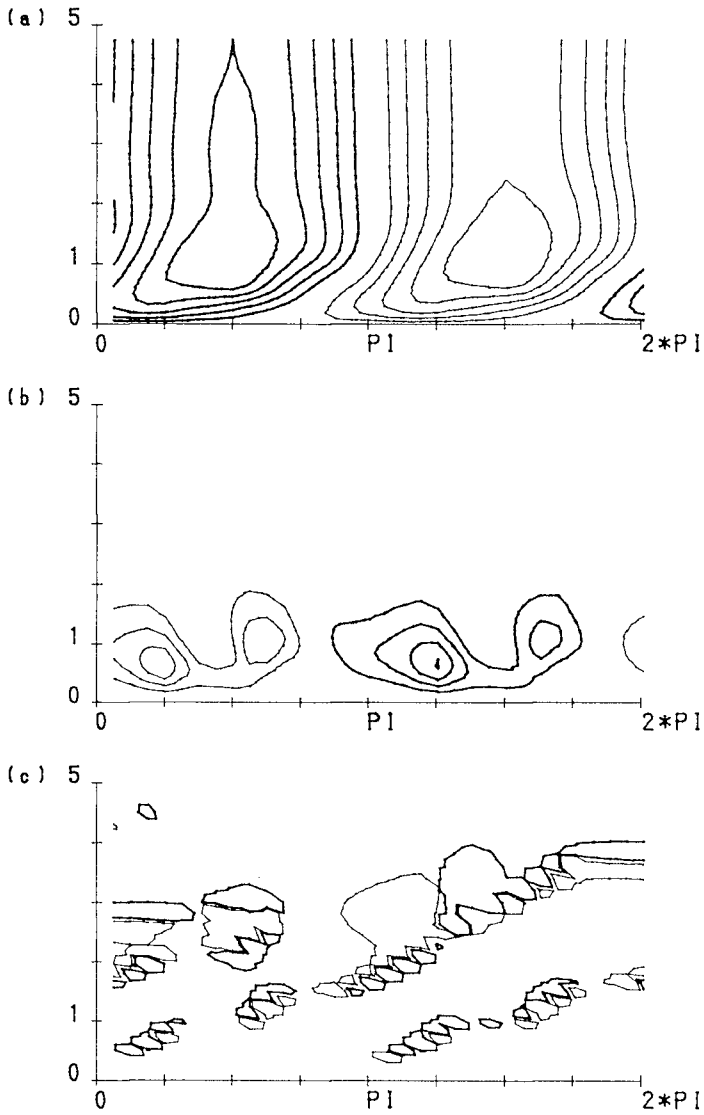   stress (Ry) (Run 23)
       (a) ~ (h) see Fig.2

(a)

(b)

(c)

Fig.9 Contours of (a) :mean fluid velocity,(b) :Reynolds stress
        and (c) :turbulent viscosity (Run 4)

(a) 5

PI   2*PI

(b) 5

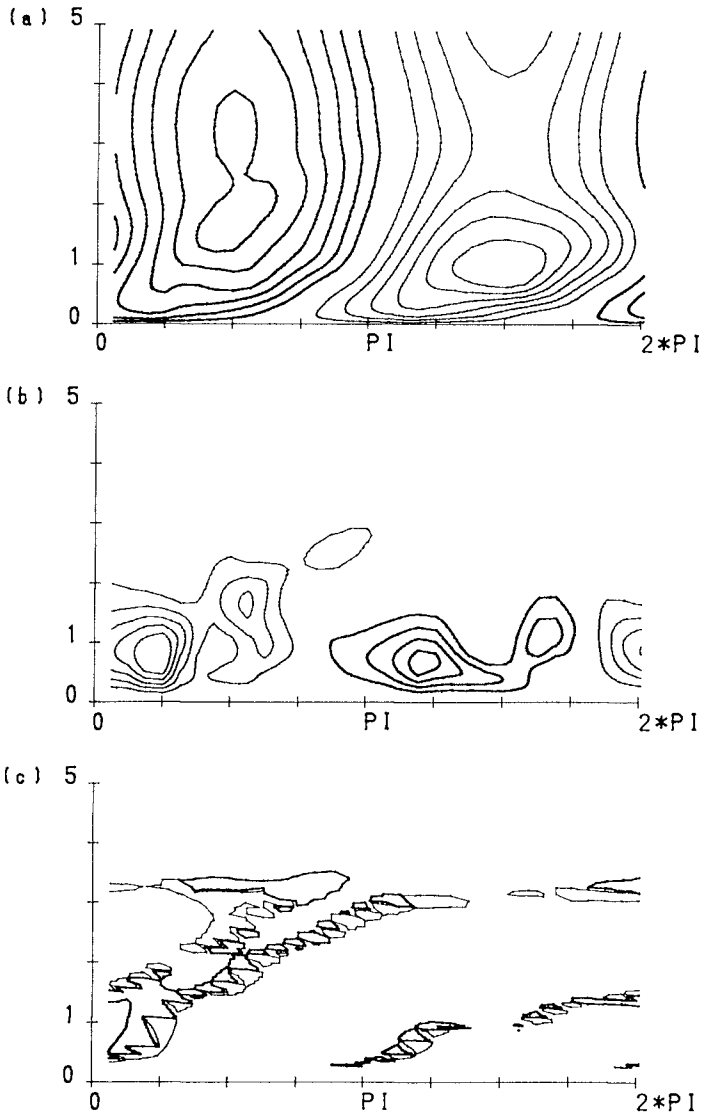PI   2*PI

(c) 5

PI   2*PI

Fig.10 Contours of (a) :mean fluid velocity,(b) :Reynolds stress
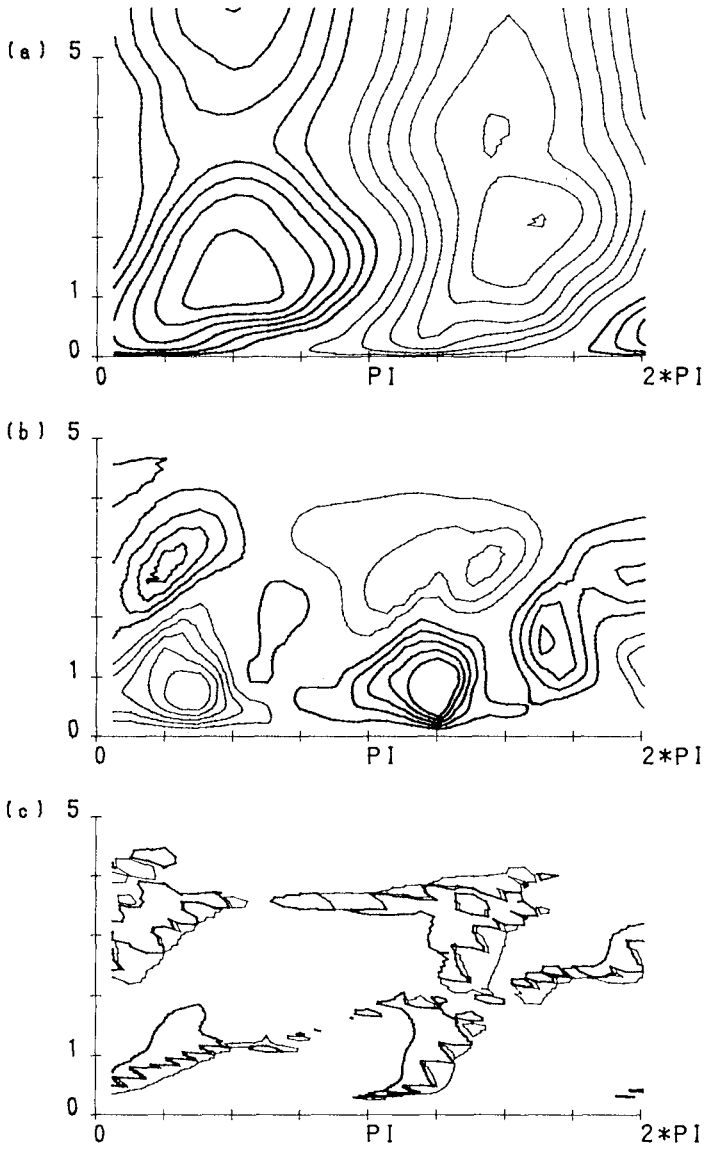   and (c) :turbulent viscosity (Run 23)

Fig.11 Contours of (a) :mean fluid velocity,(b) :Reynolds stress
and (c) :turbulent viscosity (Run 27)